

Surface-enhanced optical third-harmonic generation in Ag island films

E. M. Kim, S. S. Elvikov, T. V. Murzina, A. A. Nikulin and O. A. Aktsipetrov
Department of Physics, Moscow State University, 119992 Moscow, Russia

M. A. Bader and G. M. Arrowsky
Laser-Laboratorium Göttingen, D-37077 Göttingen, Germany
(dated: April 14, 2024)

Surface-enhanced optical third-harmonic generation (THG) is observed in silver island films. The THG intensity from Ag nanoparticles is enhanced by more than two orders of magnitude with respect to the THG intensity from a smooth and homogeneous silver surface. This enhancement is attributed to local plasmon excitation and resonance of the local field at the third-harmonic wavelength. The di- and depolarized component of the enhanced THG is associated with the third-order hyper-Rayleigh scattering in a 2-D random array of silver nanoparticles.

PACS numbers:

Observation of surface-enhanced nonlinear optical effects in silver island films dates back to two 1981 papers by Wokaun, et al., [1,2], where surface-enhanced optical second-harmonic generation (SHG) and surface-enhanced Raman scattering (SERS) were observed in silver island films. The enhancement of the SHG intensity by up to three orders of magnitude was attributed in [1] to the resonant enhancement of the local field at the second-harmonic (SH) wavelength, mediated by the excitation of the local surface plasmons in silver nanoparticles. This plasmon mechanism of the local field enhancement, introduced by Berreman [3] and Moskovits [4], was intensively discussed in the context of SERS active structures and surface-enhanced SHG from electrochemically roughened silver surfaces [5] and rough surfaces of other metals [6]. According to this approach, nonlinear polarization of a rough metal surface or an array of small metal particles is given by: $P_{2\omega} = L_{2\omega}^{(2)}(2!)L_{\omega}^2 E_{\omega}^2$ at the SH wavelength and $P_{3\omega} = L_{3\omega}^{(3)}(3!)L_{\omega}^3 E_{\omega}^3$ at the third-harmonic (TH) wavelength, where $L_{\omega}^{(2)}(2!)$ and $L_{\omega}^{(3)}(3!)$ are the second- and third-order susceptibilities of metal, respectively; E_{ω} is the optical field at fundamental wavelength; and L_{ω} , $L_{2\omega}$ and $L_{3\omega}$ are the local field factors at the corresponding wavelengths.

The spectral dependence of the local field factor of an array of small metal spheroids embedded in a dielectric matrix within the simple approach in dipole and effective media approximations, is given by [7]:

$$L(\omega) = \frac{\epsilon_d(\omega)}{\epsilon_d(\omega) + [\epsilon_m(\omega) - \epsilon_d(\omega)](N - q/3)}; \quad (1)$$

where $\epsilon_d(\omega)$ and $\epsilon_m(\omega)$ are the dielectric constants of the dielectric matrix and of the metal, respectively; N is the shape-dependent depolarization factor of the spheroids; and q is the filling factor, i.e., the relative fraction of the metal in a composite material. The resonant wavelength of the local field factor, ω_{res} , corresponds to set-

ting the real part of the denominator in Eq. 1 to zero: $\text{Re}[\epsilon_d(\omega_{res}) + [\epsilon_m(\omega_{res}) - \epsilon_d(\omega_{res})](N - q/3)] = 0$. For an isolated small Ag sphere in vacuum $\omega_{res} = 200 \text{ nm}$. Three factors result in the red-shift of ω_{res} up to the visible range for an array of particles: (1) the distortion of the particle shape, (2) the dipole-dipole interaction between particles and, (3) an increase in the dielectric constant of the matrix material. The resonant increase of the local field factor at ω_{res} results in a many-fold increase of the nonlinear-optical response from a nanoparticle array.

Up to the present time, the experimental studies of local plasmon enhancement in island films were restricted to SERS and SHG. Fig. 1d, taken from [1], shows the dependencies of the local field factor in Ag island films on mass thickness, $d_m = m/\rho$, where m is the mass of metal deposited per unit area and ρ is the bulk density of Ag. These dependencies show the maximum at $d_m = 2.0 \text{ nm}$ and $d_m = 6.0 \text{ nm}$ for wavelengths of 532 nm and 1064 nm, respectively. The decrease of d_m results in the blue-shift of ω_{res} due to a decrease of interparticle interaction. One might anticipate that the resonance at THG wavelength $\omega_{res} = 355 \text{ nm}$ for the 1064 nm fundamental wavelength can be attained for $d_m \sim 1 \text{ nm}$.

Another peculiarity of the surface-enhanced SHG from metal island films is the di- and depolarized nature of the SH radiation [5,6]. This is a manifestation of the second-order hyper-Rayleigh scattering. Silver island films are random arrays of nanoparticles which possess random spatial inhomogeneity of nonlinear susceptibilities [8] and local field factors [9]. This inhomogeneity is the source of the di- and depolarized SHG radiation in hyper-Rayleigh scattering.

The enhancement and di- and depolarized nature observed, up to now, for SHG are general features of the nonlinear optical effects in island films and are supposed to be observed in THG. Meanwhile, in spite of this analogy, there is a principle difference between SHG and THG in metal nanoparticles: $L_{\omega}^{(2)}$ is localized at the surface of nanoparticles and vanishes in the bulk of a centrosymmetric metal, whereas $L_{\omega}^{(3)}$ is a bulk localized nonlinearity [10], as shown schematically in the inset in Fig. 1a.

In this paper, surface-enhanced THG and third-order

Electronic address: aktsip@shg.ru

hyper-Rayleigh scattering is observed in Ag island films. The resonant plasmon mechanism of the THG enhancement is proved.

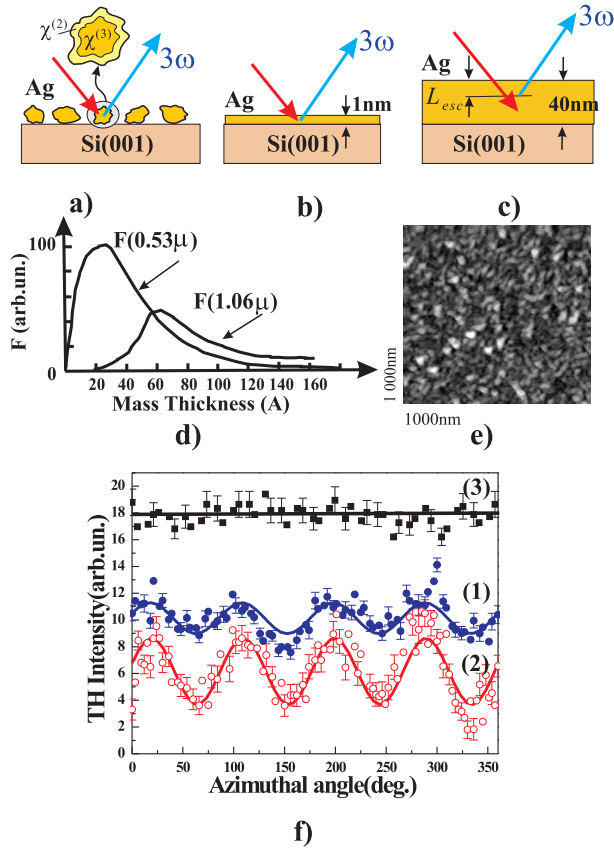


FIG. 1: Schematics of a) silver island film (inset in (a) shows the localization of $\chi^{(2)}$ and $\chi^{(3)}$ in nanoparticles); b) model of homogeneous film of the equivalent thickness of 1 nm; c) homogeneous reference Ag film with a thickness of 40 nm and an escape depth of $L_{esc} = 7$ nm for the TH wave at the fundamental wavelength $\lambda = 1064$ nm; d) dependencies of the local field factors at wavelengths of 1.064 μ m and 0.532 μ m on the mass thickness (from [1]); e) the AFM image of silver island film; f) the THG intensity as a function of the azimuthal angle from: (1) silver island film on Si(001) substrate, (2) silver-free Si(001) substrate, (3) homogeneous reference Ag film with a thickness of 40 nm; the solid lines are results of approximations.

The films were prepared by thermal evaporation of silver onto the substrates of silicon Si(001) wafers at a rate of 3-4 Å/s and residual pressure of 10^{-5} Torr. The silicon wafers were chosen as substrates because of, first, the flatness and homogeneity of the surface, and, second, the simplicity of the chemical etching procedure that is used for the preparation of a step-like SiO₂ wedge (see the scheme in Fig. 2b). Three types of Ag films are studied:

Ag island film with a mass thickness of $d_m = 1$ nm and expected plasmon resonance at $\lambda_{res} = 355$ nm, Ag island film with plasmon resonance in the vicinity of $\lambda_{res} = 270$ nm on the silicon oxide step-like wedge, and a thick homogeneous Ag reference film with a thickness of 40 nm. The thick homogeneous Ag film is used as a reference source of non-enhanced bulk THG for the measurement of the THG enhancement from island films. An atomic force microscopy (AFM), in the constant force mode, and with a height resolution of 1 nm and lateral resolution of approximately 10 nm, is used to characterize the morphology of the samples. Fig. 1e shows the AFM image of Ag island film. A cross-section of the profile shows that the average lateral size and height of silver nanoparticles is about 40 nm and 3 nm, respectively.

The outputs of two laser systems are used as the fundamental radiation in the THG and SHG experiments: (1) an OPO laser system, "Spectra-Physics 710," with a wavelength which is tunable in the spectral range from 490 nm to 680 nm, a pulse duration of 4 ns, and a pulse intensity of 2 MW/cm^2 ; and (2) a Q-switched YAG Nd³⁺ laser tuned to a 1064 nm wavelength, a pulse duration of 15 ns, and a pulse intensity of about 1 MW/cm^2 . The TH (SH) radiation is filtered out by appropriate UV and BG color and bandpass filters and detected by a PMT and gated electronics. To normalize the THG (SHG) intensity over the OPO and YAG Nd³⁺ laser fluency, and the spectral sensitivity of the optical detection system, a reference channel is used with a Z-cut quartz plate as a nonlinear optical reference and with a detection system identical to that of the "sample" channel. Polar rotation of the detector system enables us to measure the linear Rayleigh scattering pattern and the THG and SHG scattering patterns (see Fig. 2a).

In order to observe and measure an enhancement in THG, two experimental points have to be taken into account: (1) the THG signal from Ag island film should be distinguished from the Si(001) substrate contribution and (2) the THG intensity should be integrated over the diffuse THG scattering pattern. The following paragraphs focus on these points.

The curve (1) in Fig. 1f shows the azimuthal dependence of the THG intensity from the sample of Ag island film in the specular direction for the s-in, s-out combination of polarizations of the fundamental and TH waves. The anisotropic component of the THG signal is related to the nonlinear response of Si(001) substrate, whereas the isotropic THG is attributed to both Ag nanoparticles and Si substrate. To distinguish the THG contribution of Ag island film from that of the substrate, the azimuthal dependence of the THG intensity from Si(001) is measured in the same s-in, s-out geometry (curve (2) in Fig. 1f). The ratio of the anisotropic components of THG from silver island film on Si(001), $I_{F+Si}^{anis}(3!)$, and silver-free Si(001) substrate, $I_{Si}^{anis}(3!)$, gives an attenuation coefficient of the THG response from substrate due to the absorption and scattering in the silver coverage: $\beta_{3!} = I_{F+Si}^{anis}(3!)/I_{Si}^{anis}(3!) = 0.46$. The estimation of the $\beta_{3!}$

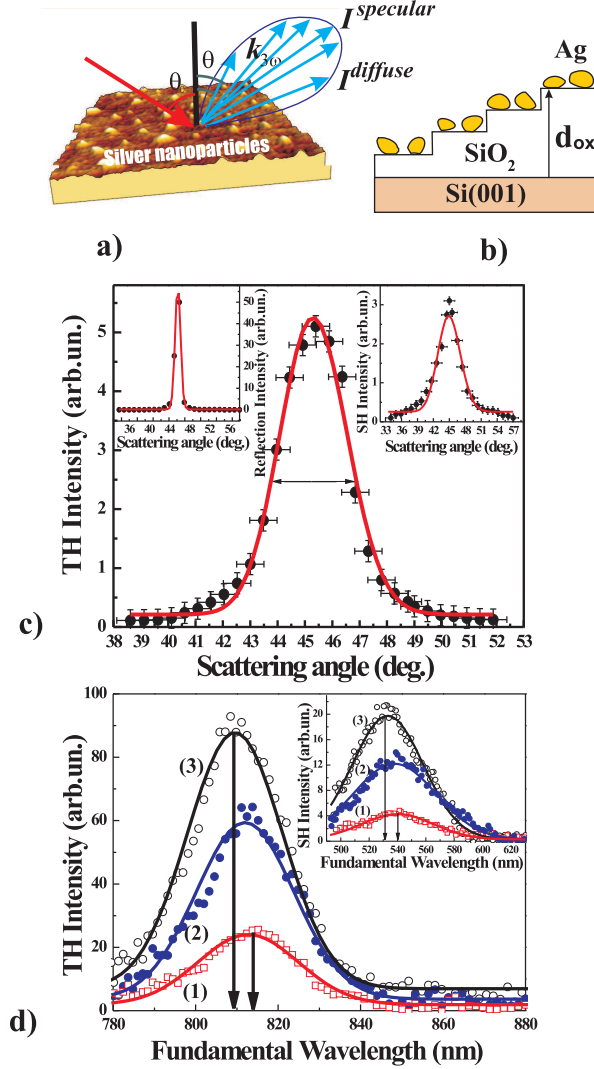


FIG. 2: a) The scheme of the hyper-Rayleigh scattering experiment; b) scheme of silicon oxide step-like wedge as a variable spacer between the island film and the high-dielectric constant material (silicon); d_{ox} is the thickness of the silicon oxide steps; c) THG scattering pattern: the THG intensity from the island film as a function of polar scattering angle (angular width is $3^\circ \pm 0.5^\circ$); left inset is the linear Rayleigh scattering pattern, with angular width of $1^\circ \pm 0.5^\circ$; right inset is the SHG scattering pattern, with angular width of $5^\circ \pm 0.5^\circ$; solid lines are approximations with Eq. 3; d) main panel: dependencies of the THG intensity on the fundamental wavelength for Ag island films deposited on the SiO_2 step-like wedge for $d_{ox} = 2$ nm (1), 70 nm (2) and 100 nm (3); inset: the same for the SHG intensity spectra; solid lines are approximations by Gaussian function.

coefficient is the first step in the determination of the THG enhancement for Ag island films. The relative value of the THG intensity from Ag nanoparticles in the specular direction is $I_{IF}^{spec}(3!) = I_{IF+Si}^{is}(3!) - 3! I_{Si}^{is}(3!)$, where $I_{IF+Si}^{is}(3!)$ and $I_{Si}^{is}(3!)$ are the isotropic components of THG from the island film on $\text{Si}(001)$ and from silver-free substrate, respectively. Obtaining the total intensity of the diffuse THG from Ag nanoparticles is the second step in the determination of the THG enhancement. This demands the measurement of the THG scattering pattern which is dependent on the diffuse THG intensity, which in turn depends on the polar scattering angle: $I_{IF}(3!; \theta) = I_{IF}^{spec}(3!) S_{3!}(\theta)$, where θ and $S_{3!}(\theta)$ are the polar scattering angle and the normalized form-factor of the third-order hyper-Rayleigh scattering, respectively. The main panel in Fig. 2c shows the experimental scattering pattern of diffuse THG from silver island films where the angular width of the normalized form-factor is approximately $3^\circ \pm 0.5^\circ$. This sufficiently exceeds the angular width of $1^\circ \pm 0.5^\circ$ of the scattering pattern of linear Rayleigh scattering from the same silver island film presented in the left inset in Fig. 2c, whereas the angular width of the SHG scattering pattern is approximately $5^\circ \pm 0.5^\circ$. The total intensity of the diffuse THG can be obtained by angular integration of the THG scattering pattern and in the case of the small angular width of $S_{3!}(\theta)$, is given by: $I_{IF}(3!) = I_{IF}^{spec}(3!) \left[\frac{1}{\Delta\theta} \int_{\theta_1}^{\theta_2} S_{3!}(\theta) d\theta \right] \approx 0.6 \pm 0.1 I_{IF}^{spec}(3!)$, where

$\Delta\theta$ is an angular aperture of the THG detection system and $\int_{\theta_1}^{\theta_2} S_{3!}(\theta) d\theta$ is the angular interval of integration. To estimate quantitatively the THG enhancement, we consider the total THG intensity of the specular THG from a model homogeneous film with an equivalent thickness of $d_{eq} = 1$ nm and compare this with the THG intensity from a reference film with a thickness of 40 nm (see Fig. 1b and c). The THG intensity detected from the reference film comes from the Ag layer corresponding to the escape depth L_{esc} of the TH wave (curve (3) in Fig. 1f). In our experimental conditions, $L_{esc} = 7$ nm for $\lambda = 355$ nm. Thus, the enhancement of the THG intensity from Ag island film with respect to a thick homogeneous Ag film is given by:

$$G = \frac{I_{IF}(3!)}{I_{ref}(3!)} = \frac{R_{40} \int_0^{R_{40}} \exp(-(\beta_1 + 3\beta_2)r) dr}{\int_0^{R_{40}} \exp(-(\beta_1 + 3\beta_2)r) dr} \approx 1.2 \pm 0.2; \quad (2)$$

where $I_{ref}(3!)$ is the THG intensity from reference Ag film, β_1 and β_2 are adsorption coefficients at the fundamental and TH wavelengths, respectively, and r is coordinate normal to the film surface.

To prove the plasmon assistance in the THG enhancement, the dependencies of the THG intensity on the fundamental wavelength are studied for Ag island films deposited onto a step-like SiO_2 wedge on silicon wafer. Silicon oxide steps serve as variable spacers between the silver nanoparticles and silicon substrate, which is a high-

dielectric constant material. Variations of SiO_2 thickness, d_{ox} , result in the variations of the effective dielectric constant $\epsilon_{\text{dl}}(d_{\text{ox}}) = \epsilon_{\text{dl}}^0(d_{\text{ox}}) + i\epsilon_{\text{dl}}^{\text{im}}(d_{\text{ox}})$ in Eq. 1: the increase of d_{ox} corresponds to the decrease of the effective $\epsilon_{\text{dl}}(d_{\text{ox}})$. Theoretical modeling [11] shows that the decrease of the real part, $\epsilon_{\text{dl}}^0(d_{\text{ox}})$, results in the blue-shift of the resonant plasmon wavelength, whereas the decrease of the imaginary part, $\epsilon_{\text{dl}}^{\text{im}}(d_{\text{ox}})$, leads to the enhancement of the local field amplitude.

The main panel in Fig. 2d shows a set of THG spectra for d_{ox} increasing in the range from 2 nm to 100 nm. The observed effects of d_{ox} on the THG spectra as SiO_2 thickness increases from 2 nm to 100 nm is two-fold: (1) an apparent blue-shift of approximately 6 nm of the THG resonance and, (2) a more than four-fold increase of the THG resonant intensity. These changes correspond to the decrease of the effective dielectric constant of Ag islands situated at different steps of the SiO_2 wedge. An analogous blue-shift of about 10 nm and manyfold increase of the resonant SHG intensity are observed in the same conditions (refer to the inset in Fig. 2d). The impact of the dielectric constant of the substrate on the resonant properties of surface-enhanced THG and SHG proves the plasmon-assisted mechanism of the enhancement. A slight difference in the spectral shift for THG and SHG can be associated with the different localizations of (3) and (2) in metal nanoparticles. Moreover, different spatial localizations of nonlinear susceptibilities in metal particles can result in different parameters of scattering patterns at the TH and SH wavelengths from a random array of Ag nanoparticles. Normalized form-factors at the TH and SH wavelengths are given by:

$$S_{3!;2!}(\theta) = \exp[-M_{3!;2!} k_{3!;2!}^2 l_{\text{cor}}^2(3!;2!)] \quad (3)$$

where $l_{\text{cor}}(3!;2!)$ is the correlation length at the TH and SH wavelengths, respectively, $k_{3!;2!} = 2(\sin \theta)/\lambda_{0(3!;2!)}$ and $M_{3!;2!}$ is an adjustable parameter at the TH and SH wavelengths, respectively; and θ_0 is the angle of incidence. The approximation of the diffuse THG and SHG scattering patterns (Fig. 2c, solid lines) by Eq. 3 corresponds to the correlation lengths of $l_{\text{cor}}(3!) = 42$ nm and $l_{\text{cor}}(2!) = 20$ nm. The former probably corresponds to the average Ag particle size of 40 nm obtained from the AFM measurements because of the bulk localization of (3) . Meanwhile, the latter being twice as small as $l_{\text{cor}}(3!)$, corresponds to the smaller scale of the (2) inhomogeneity due to its surface localization within the individual particles.

In conclusion, surface-enhanced THG is observed in Ag island films with an enhancement of 1.2×10^4 which is attributed to the local surface plasmon excitation in Ag nanoparticles at the TH wavelength. Usefulness of surface-enhanced THG allows us to associate this effect with the third-order hyper-Rayleigh scattering in a random array of nanoparticles. The difference in scattering patterns and spectroscopic resonances between surface-enhanced THG and SHG can be attributed to the different localizations of (3) and (2) in nanoparticles.

Acknowledgments

This work is supported in part by the Russian Foundation for Basic Research (Grants No. 04-02-16847, 04-02-17059, 03-02-39010), the Presidential Grants for Leading Russian Science Schools (No. 1604.2003.2 and 1909.2003.2), the DFG Grant No. 436 RUS 113/640/0-1, the NATO Grant PST CLG .979406 and the INTAS Grant No. 03-51-3784.

-
- [1] A. Wokaun, J.G. Bergman, J.P. Heritage, A.M. Glass, P.F. Liao and D.H. Olson, Phys. Rev. B. 24, 849 (1981).
 - [2] A. Wokaun, J.P. Gordon and P.F. Liao, Chem. Phys. Lett. 48, 957 (1981).
 - [3] D.W. Berreman, Phys. Rev. 163, 855 (1967).
 - [4] M. Moskovits, J. Chem. Phys. 69, 4159 (1978).
 - [5] C.K. Chen, A.R.B. de Castro and Y.R. Shen, Phys. Rev. Lett. 46, 145 (1981).
 - [6] G.T. Boyd, Th. Rasing, J.R.R. Leite and Y.R. Shen, Phys. Rev. B. 30, 519 (1984).
 - [7] V.I. Emelyanov, N.I. Koroteev, Soviet Fiziks-Uspkhi, 135, 345 (1981).
 - [8] O.A. Aktsipetrov, P.V. Elyutin, A.A. Nikulin and E.A. Ostrovskaya, Phys. Rev. B. 51, 17 591-599, (1995).
 - [9] M. Breit, V.A. Podolsky, S.G. Resillon, G. von Plessen, J. Feldman, J.C. Rivoal, P. Gadenne, V.M. Shalaev, A.K. Sarychev, Phys. Rev. B. 64, 125106-1, (2001).
 - [10] N. Bloembergen, R.K. Chang, S.S. Jha, C.H. Lee, Phys. Rev. 147, 813-822, (1968).
 - [11] O.A. Aktsipetrov, E.M. Dubinina, S.S. Elvnikov, E.D. Mishina, A.A. Nikulin, N.N. Novikova, M.S. Strelkov, Sol. Stat. Comm. 70, 1021-1024, (1989).